HHS Public Access

Author manuscript

Cancer Cell. Author manuscript; available in PMC 2017 July 05.

Published in final edited form as:

Cancer Cell. 2017 January 09; 31(1): 110–126. doi:10.1016/j.ccell.2016.11.010.

Molecular checkpoint decisions made by subverted vascular niche transform indolent tumor cells into chemoresistant cancer stem cells

Zhongwei Cao[1,2], **Joseph M Scandura**[3], **Giorgio G. Inghirami**[4], **Koji Shido**[1], **Bi-Sen Ding**[1,2], and **Shahin Rafii**[1,5]

[1]Ansary Stem Cell Institute, Division of Regenerative Medicine, Department of Medicine, Weill Cornell Medicine, New York, NY 10065

[2]Laboratory of Birth Defects and Related Diseases of Women and Children, State Key Laboratory of Biotherapy, West China Second University Hospital, Sichuan University, and Collaborative Innovation Center for Biotherapy, Chengdu, 610041, China

[3]Division of Hematology-Oncology, Department of Medicine, Weill Cornell Medicine, New York, NY 10065

[4]Department of Pathology and Laboratory Medicine, Weill Cornell Medicine, New York, NY 10065

Summary

Tumor-associated endothelial cells (TECs) regulate tumor cell aggressiveness. However, the "core" mechanism by which TECs confer stem cell-like activity to indolent tumors is unknown. Here, we used in vivo murine and human tumor models to identify tumor-suppressive checkpoint role of TEC-expressed insulin growth factor (IGF) binding protein-7 (IGFBP7/angiomodulin). During tumorigenesis, IGFBP7 blocks IGF1 and inhibits expansion and engraftment of tumor stem-like cells (TSCs) expressing IGF1-receptor (IGF1R). However, chemotherapy triggers TECs to suppress IGFBP7, and this stimulates $IGF1R^+$ TSCs to express FGF4, inducing a feed-forward FGFR1-ETS2 angiocrine cascade that obviates TEC IGFBP7. Thus, loss of IGFBP7 and upregulation of IGF1 activates the FGF4-FGFR1-ETS2 pathway in TECs and converts naive tumor cells to chemoresistant TSCs, thereby facilitating their engraftment and progression.

Introduction

Tumors are comprised of heterogeneous tumor and host cell populations (Chao et al., 2010; Hoey et al., 2009; Nakasone et al., 2012). Although chemotherapy can eliminate the majority of proliferating tumor cells, a subset—referred to as tumor propagating cells or tumor stem-like cells (TSC)—is believed to cause cancer relapse and death because they

*Correspondence: S.R.: srafii@med.cornell.edu; B-S D: bid2004@med.cornell.edu; Z.C.: zhc2007@med.cornell.edu;.
[5]Lead contact

Author Contributions

Z.C. designed the study, performed the experiments, interpreted the results, and wrote the paper. K.S. performed the experiments and analyzed the data. J.M.S and G.G.I analyzed the data and edited the manuscript. B.-S.D. conceived and carried out the experiments, analyzed the data and wrote the paper. S.R. designed the experiments and wrote the manuscript.

manifest higher invasiveness and resistance to chemotherapy (chemoresistance). TSCs are thought to be organized as the apex of a tumor hierarchy with all tumor cells growing from this common root. However, TSCs are not necessarily rare and the mechanisms responsible for their specialized properties are not entirely clear (Magee et al., 2012; Passegue et al., 2009; Plaks et al., 2015; Quintana et al., 2008; Schepers et al., 2015).

By definition, TSCs share genetics with co-existing, “non-stem”, indolent tumor cells but manifest their significant “stem” phenotypes under the influence of both cell-intrinsic and cell-extrinsic factors. TSCs can acquire aggressive features by interacting with specialized tumor-associated niche cells, such as vascular endothelial cells (ECs) (Bergers and Hanahan, 2008; Calabrese et al., 2007; Franses et al., 2014; Ghajar et al., 2013; Gilbert and Hemann, 2010; Hanahan and Coussens, 2012; Schmidt et al., 2011; Tavora et al., 2014). However, identifying a "core mechanism" by which tumor-associated ECs (TECs) functionalize a tumorigenic vascular niche to instigate and perpetuate cancer stem cell-like properties would simplify the development of niche-targeting therapies (Carmeliet and Jain, 2011; Weis and Cheresh, 2011).

Our group and others have shown that tissue-specific ECs provide “context-specific” trophogenic paracrine cues, known as angiocrine factors, to trigger the propagation of stem/progenitor cells during organ regeneration (Beck et al., 2011; Cao et al., 2016; Ding et al., 2014; Ding et al., 2010; Ding et al., 2011; Ding et al., 2012; Hu et al., 2014; Lu et al., 2013; Rafii et al., 2015). Indolent lymphoma cells can be interconverted to genetically identical aggressive lymphoma TSCs expressing CD44, CSF1R, and IGF1R upon activation with angiocrine factors produced by maladapted tumor ECs (TECs) (Cao et al., 2014; Medyouf et al., 2011; Trimarchi et al., 2014). Similarly, TEC expression of CXCL12 can stimulate pre-T cell acute lymphoblastic leukemia progression and gastric carcinogenesis (Hayakawa et al., 2015; Pitt et al., 2014). It is appealing to envision development of new classes of therapeutic agents that disrupt the perfusion-independent instructive TECs signals that promote aggressive tumor phenotypes. Here, we hypothesized that tumor-driven subversion of TECs deploy aberrantly programmed paracrine signals to authorize aggressive TSC phenotypes.

Results

Endothelial cells (ECs) induce IGF1R-dependent chemoresistance in TSCs

In order to eavesdrop on the crosstalk between ECs and tumor cells, we developed a serum-free system to co-culture human umbilical vein vascular ECs (HUVECs) and tumor cells (Cao et al., 2014). This approach enabled us to dissect the molecular mechanism through which naïve HUVEC feeders acquire pro-tumorigenic properties that endow chemoresistance to tumor cells. Using this tumor cell-EC co-culture system, we found that several tumor cell types—including lymphoma cells (LCs), hepatocellular carcinoma cells (HCCs), and Lewis lung carcinoma cells (LLCs)—are more resistant to doxorubicin when co-cultured with ECs than when cultured alone (Figure 1A). Thus, ECs form a niche that confers chemoresistant potential to tumor cells.

ECs enhance tumor chemoresistance by stimulating the expansion of aggressive $CD44^{+}CSF1R^{+}IGF1R^{+}$ LCs (Cao et al., 2014). Thus, we tested the functional contribution

of CD44, CSF1R, and IGF1R in establishing chemoresistant TSCs. In tested tumor cells, shRNA knockdown of *Igf1r,* but not *Cd44* or *Csf1r* or a scrambled sequence control (*Srb*), abrogated resistance to doxorubicin treatment even in the presence of EC feeders (Figure 1A). Reciprocally, adding recombinant IGF1 to serum-free medium in the absence of ECs promoted survival of tumor cells treated with doxorubicin (Figure 1B, Figure S1A). We found that other tumor cell types also induced IGF1R expression when co-cultured with ECs and expression of IGF1R was required for EC-rescue of the tumor cells from chemotherapy cytotoxicity (Figure 1C, D and Figure S1B). As such, ECs induce IGF1R expression in tumor cells and confer to them a chemoresistant phenotype.

To investigate whether IGF1R is activated in chemoresistant human tumor cells *in vivo*, we analyzed LCs isolated from patient-derived tumor xenograft (PDTX) mice after treatment with chemotherapy. Immunodeficient mice were transplanted with human T-cell LCs and treated with a murine equivalent of “CHOP” chemotherapy (cyclophosphamide, daunorubicin, vincristine, prednisolone). This PDTX mouse model allows us to study the *in vivo* response of human LCs to chemotherapy. Notably, IGF1R is preferentially expressed on the human LCs adjacent to VE-cadherin^{+} host ECs and was further upregulated in lymphoma tissues that outgrew after CHOP treatment (Figure 1E, Figure S1C). Thus, IGF1R is enriched in perivascular human LCs and is induced in chemotherapy resistant cells.

We then sought to unravel the mechanism whereby IGF1R confers chemotherapy resistance to tumor cells. Apoptosis and proliferation in LC transduced with scrambled sequence (LC^{Srb}) or *Igf1r* shRNA (LC^{shIGF1R}) were compared. Both LC^{Srb} and LC^{shIGF1R} were intrasplenically transplanted into mice, and recipient mice were treated with chemotherapy. TUNEL assay showed that TECs prevented tumor cell death from chemotherapy in LC^{Srb}, but not LC^{shIGF1R}, localized in the proximity of the blood vessels (Figure 1F, Figure S1D). Additionally, inhibitor of PI3K-Akt pathway reduced the chemoresistance of LCs (Figure S1E). Thus, induction of IGF1R by TECs in LCs stimulates Akt-activation to enhance cell survival after doxorubicin treatment. By contrast, there was no significant difference between cell proliferation in these two LC groups, as indicated by Ki67 staining (Figure 1G, Figure S1F). Therefore, EC-driven IGF1R signaling in LCs provokes TSC-activity, such as chemoresistance by enhancing cell survival rather than promoting cell proliferation.

Next, the mechanism by which IGF1R conferred *in vivo* chemoresistance to tumor cells was determined. Different types of tumor cells, including LCs, HCCs and LLCs, were transduced with scrambled sequence (tumor cell: TC^{Srb}) or shRNA for *Igf1r* (TC^{shIGF1R}), and both TC^{Srb} and TC^{shIGF1R} were intraperitoneally (i.p.) or intravenously (i.v.) injected into wild type mice to assess the *in vivo* tumorigenicity. The response of recipient mice to chemotherapy was also tested. IGF1R knock down chemosensitized all three different tumor cell types and prolonged survival of recipient mice in combination with chemotherapy (Figure 1H).

IGF1R-dependent chemoresistance of tumor cells was then tested in different organs. *Igf1r* gain and loss of function study was performed in isolated IGF1R^{+} and IGF1R^{-} tumor cells (Figure 1I). LCs and HCCs were transplanted into the mouse liver by an intrasplenic

injection model (Cao et al., 2014), and LCs and LLCs were transplanted into the mouse lung by intravenous injection. Recipient mice were treated with doxorubicin. Knocking down IGF1R in IGF1R^{+} tumor cells attenuated hepatic and pulmonary tumor load in the recipient mice after doxorubicin treatment, to an extent comparable to that of indolent IGF1R^{-} tumor cells (Figure 1J, Figure S1G, H). Reciprocally, enforcing IGF1R expression in IGF1R^{-} tumor cells elevated tumor load in both liver and lung of treated mice. Thus, IGF1R confers *in vivo* chemoresistant TSC features to tumor cells.

IGF1 expressed by TECs stimulates chemoresistance in IGF1R^{+} TSCs

The essential role of EC feeders in generating chemoresistant IGF1R^{+} TSCs led us to search for IGF1R-ligand expressed by ECs. Since ECs in different vascular beds supply unique tissue-specific angiocrine factors (Rafii et al., 2016), including IGF1R-ligands (Nolan et al., 2013), we co-cultured LCs with mouse ECs isolated from different organs, including pancreas, thymus, lung and liver. Co-culturing with mouse liver ECs induced the most efficient LC expansion**,** with the highest tolerance to doxorubicin treatment (Figure 2A, Figure S2A). As such, we compared the expression level of IGF1, the most efficient IGF1R agonist, in the ECs. Indeed, liver ECs expressed significantly more IGF1 than ECs from other organs (Figure 2B). Notably, silencing IGF1R in LCs or co-culturing LCs with IGF1-deficient ECs abolished the vascular niche stimulated chemoresistance (Figure 2C), implicating over-supply of IGF1 by liver ECs in the chemoresistant phenotype of co-cultured LCs.

We used an inducible genetic mouse model to investigate the function of IGF1 in promoting chemoresistance *in vivo* (Figure 2D). *Igf1* was deleted in ECs of adult mice (*Igf1*$^{i\Delta EC/i\Delta EC}$) by VE-cadherin-driven tamoxifen-responsible Cre (VE-cadherin-Cre^{ERT2}). LCs and HCCs were i.p. injected into mice with EC-specific deletion of *Igf1* (*Igf1*$^{i\Delta EC/i\Delta EC}$) or control mice (*Igf1*$^{i\Delta EC/+}$). Similarly, LLCs were i.v. injected into *Igf1*$^{i\Delta EC/i\Delta EC}$ and control animals. Recipient mice were then treated with or without doxorubicin to assess the *in vivo* response to chemotherapy. Survival of *Igf1*$^{i\Delta EC/i\Delta EC}$ mice transplanted with all three types of tumor cells was significantly prolonged compared to control mice. Injection of IGF1-overexpressing tumor cells reversed the phenotype of *Igf1*$^{i\Delta EC/i\Delta EC}$ mice (Figure S2B). As such, IGF1-derived from ECs plays an essential role in endowing chemoresistance to tumor cells.

We further dissected the effect of endothelial-IGF1 on the organ-specific response of TSCs to various chemotherapeutic agents. LCs and HCCs were transplanted into the liver of *Igf1*$^{i\Delta EC/i\Delta EC}$ or control *Igf1*$^{i\Delta EC/+}$ mice, and LCs and LLCs were also i.v. injected into *Igf1*$^{i\Delta EC/i\Delta EC}$ or control mice. After treatment with doxorubicin, 5-fluorouracil (5-FU), and cisplatin, tumor localization in the liver and lung was analyzed. Genetic deletion of *Igf1* in ECs significantly reduced tumor load in both the liver and lung following all tested types of chemotherapy regimens (Figure 2E, Figure S2C, D). Tumor cells isolated from *Igf1*$^{i\Delta EC/i\Delta EC}$ mice after chemotherapy showed substantially lower IGF1R activation compared to tumor cells engrafted in control *Igf1*$^{i\Delta EC/+}$ mice (Figure 2F). Hence, IGF1 expressed by TECs instigates the chemoresistance in tumor cells possibly via activating IGF1R^{+} TSCs.

TECs express IGF1R antagonist IGFBP7 to constrain chemoresistance in TSCs

IGF binding proteins (IGFBPs) modulate IGF1R signaling (Chen et al., 2013; Evdokimova et al., 2012; Verhagen et al., 2014; Wajapeyee et al., 2008) and ECs express IGFBPs that could modulate IGF1R-dependent chemoresistance in tumor cells. For these reasons, we compared the effects of IGFBPs on IGF1R-mediated chemoresistance in LCs. Among all tested IGFBPs, IGFBP7 decreased chemoresistance in LCs co-cultured with ECs (Figure 3A–B, Figure S3A). Immunoprecipitation demonstrated that IGFBP7, but not other IGFBPs, bound to IGF1R and blocked its activation/phosphorylation in the presence of IGF1 (Figure 3C. D). Accordingly, IGFBP7 recombinant protein reduced TSC activity, such as colony formation ability in LCs, whereas overexpressing IGF1R in LCs restored this activity (Figure S3B).

To test the *in vivo* effects of IGFBP7 on modulating TSC features, $IGF1R^+$ LCs, HCCs, and LLCs were i.p. or i.v. transplanted into mice, and recipient mice were treated with IGFBP7 (Figure 3E). IGF1R activity/phosphorylation in isolated $IGF1R^+$ tumor cell was markedly decreased by IGFBP7 (Figure 3E–G). Mouse lethality was subsequently compared in recipient mice after IGFBP7 injection with or without doxorubicin. For tumor cell transplantation, IGF1R was silenced by shRNA in LCs, HCCs, and LLCs (shIGF1R) and compared with scrambled sequence (Srb)-transduced tumor cells. Mice transplanted with shIGF1R-transduced tumor cells survived significantly longer compared with mice engrafted with Srb-transduced $IGF1R^+$ tumor cells. In the presence of doxorubicin, IGFBP7 treatment increased survival of mice transplanted with $IGF1R^+$ tumor cells, but not tumor cells lacking IGF1R (Figure 3H). Of note, decreased tumor load in $Igf1^{i\Delta EC/i\Delta EC}$ mice or after IGFBP7 treatment was not associated with perturbation of vascular perfusion (Figure S3C). As such, IGFBP7 inhibits IGF1R-dependent and angiocrine-driven chemoresistance in $IGF1R^+$ TSCs.

Since IGFBP7 is preferentially induced in TECs (St Croix et al., 2000), we postulated that IGFBP7 might serve as an angiocrine tumor suppressor. To define the chemoresistance-suppressive capacity of IGFBP7 *in vivo*, IGFBP7 expression was analyzed in the mouse liver and lung injected with LCs, HCCs, or LLCs. Indeed, IGFBP7 expression was significantly elevated in both hepatic and pulmonary ECs after tumor cell transplantation, suggesting that TECs express IGF1R-inhibitory factor to dampen the aggressive features of $IGF1R^+$ TSCs (Figure 3I, Figure S3D–G). Of note, expression of IGFBP7 in TECs was strongly reduced in both liver and lung after treatment with doxorubicin, implicating IGFBP7 as a paracrine checkpoint in TECs that is suppressed in chemoresistant tumor.

To determine the functional contribution of host IGFBP7 in abrogating tumor chemoresistance, we employed *Igfbp7* knock out ($Igfbp7^{-/-}$) mice (Hooper et al., 2009). LCs, HCCs, and LLCs were i.p. or i.v. transplanted into WT ($Igfbp7^{+/+}$) or $Igfbp7^{-/-}$ mice and treated with doxorubicin. Survival of $Igfbp7^{-/-}$ mice was lower than wild type control in the presence of chemotherapy (Figure 4A). Of note, administration of IGFBP7 in conjunction with doxorubicin drastically prolonged the life span of both WT and $Igfbp7^{-/-}$ mice. Decreased survival of tumor-carrying $Igfbp7^{-/-}$ mice was accompanied by elevated load of chemoresistant tumor in the liver and lung (Figure 4B, Figure S4A), and higher degree of IGF1R activation in tumor cells (Figure 4C–D, Figure S4B). Notably, injection of IGF1R neutralizing antibody similarly prolonged the life span of both WT and $Igfbp7^{-/-}$

mice after chemotherapy (Figure 4E, Figure S4C). Therefore, loss of suppressive IGFBP7 in TECs promotes activation of IGF1R signaling in chemoresistant TSCs and recurrence of an aggressive tumor.

FGF4 derived from aggressive TSCs stimulates FGFR1 in TECs to balance IGF1 and IGFBP7 expression

We then dissected the molecular mechanisms governing the balance between tumorigenic IGF1 and tumor-restricting IGFBP7 in TECs. Several growth factors that might induce endothelial cell activation were tested. Transcriptional levels of vascular endothelial growth factor-A (VEGF-A), stromal derived factor-1 (SDF-1 or CXCL12), fibroblast growth factors (FGFs) were examined in tumor cells co-cultured with endothelial cell (Figure 5A). FGF4 was the most upregulated factor in tumor cells by doxorubicin, 5-FU and cisplatin chemotherapy (Figure 5A–B). We then identified canonical Wnt signaling as an upstream pathway stimulating FGF4 induction in tumor cells by doxorubicin because knockdown of β-catenin in tumor cells suppressed FGF4 expression after doxorubicin treatment (Figure 5C, D). As such, stress induced by chemotherapeutic agents activates canonical Wnt-β-catenin to selectively upregulate FGF4 in tumor cells.

To further assess the role of FGF4 in the crosstalk between tumor cells and ECs *in vivo*, we silenced *Fgf4* in LCs, HCCs and LLCs with shRNA (Figure S5A), engrafted these FGF4-deficient tumor cells into mouse liver and lung, and subsequently treated the recipient mice with chemotherapy. shRNA-mediated FGF4 knockdown in tumor cells reduced activation of several downstream effectors of FGF-receptor in neighboring TECs (Figure 5E, Figure S5B). Importantly, IGF1 expression was reduced and IGFBP7 expression was increased in TECs adjacent to tumor cells lacking FGF4 (Figure 5F–G). This data implicates tumor cell-derived FGF4 as a key arbiter of the IGF1/IGFBP7 balance in TECs.

We then sought to identify the FGF-receptor (FGFR) relaying FGF4 signaling in TECs. We again used shRNA to silence FGFR1 or FGFR2 in HUVECs and then co-cultured the deficient ECs with isolated $IGF1R^+$ LCs, HCCs, and LLCs. Knockdown of *Fgfr1*, but not *Fgfr2*, altered the expression of IGF1 and IGFBP7 in HUVECs after incubation with $IGF1R^+$ TSCs (Figure 5H). Therefore, aggressive TSCs produce FGF4 that signals through FGFR1 on TECs to upregulate IGF1 and suppress IGFBP7.

To examine the *in vivo* function of endothelial-supplied *Fgfr1* in promoting chemoresistance, mice with EC-specific deletion of *Fgfr1* (*Fgfr1*$^{i\Delta EC/i\Delta EC}$) were transplanted with LCs, HCCs, LLCs. *Fgfr1*$^{i\Delta EC/+}$ mice were used as control. Recipient mice were treated with doxorubicin or vehicle. Deletion of *Fgfr1* in ECs decreased IGF1 expression and increased IGFBP7 expression in TECs in liver and lung tumors after chemotherapy (Figure 6A–B). After chemotherapy, tumor cell-engrafted *Fgfr1*$^{i\Delta EC/i\Delta EC}$ mice lived much longer than control mice (Figure 6C, Figure S6A). In addition, IGF1R protein expression and activation in isolated tumor cells were drastically decreased in recipient *Fgfr1*$^{i\Delta EC/i\Delta EC}$ mice, compared to the control group (Figure 6D). Hence, activation of FGFR1 pathway in TECs suppresses the IGF1R antagonist IGFBP7 and upregulates IGF1 (Figure 6E).

Next, we hypothesized that FGF4 activation of FGFR1 on the TECs will induce aggressive features in indolent tumor cells. To test this, FGF4 was i.p. administered into mice one day before limiting dilution transplantation of IGF1R$^+$ TSCs and every three days thereafter. FGF4 injection to host mice enhanced the lethality of all transplanted TSCs (Figure 6F). On average, treatment with FGF4 allowed 100-fold fewer tumor cells to kill the recipient mice compared to controls. Of note, FGF4-enhanced tumor cell lethality was abolished in *Fgfr1*$^{i\Delta EC/i\Delta EC}$ mice, suggesting that the TSC-enabling effect of FGF4 acts via activation of endothelial FGFR1 expressed in host mice (Bono et al., 2013) (Figure S6B).

FGFR1-ETS2 axis modulates IGF1/IGFBP7 expression in TECs

The effect of FGF4-FGFR1 axis in subverting the tumor vascular niche led us to investigate how endothelial FGFR1 affects the IGF1/IGFBP7 checkpoint hub. E26 transformation-specific (ETS) family transcription factors modulate the behavior of both tumor cells and associated microenvironmental cells (Phan et al., 2013). Thus, we first compared the expression of ETS family transcription factors in naïve HUVECs co-cultured with LCs, HCCs, and LLCs. ETS2 was preferentially upregulated in HUVECs by both co-culture with tumor cells or FGF4 stimulation (Figure 7A–D), and genetic silencing ETS2 in HUVECs by shRNA abolished IGF1 upregulation and prevented IGFBP7 suppression in stimulated HUVECs (Figure 7E–G). Therefore, induction of ETS2 dictates the balance of IGF1 relative to IGFBP7 in TECs.

In contrast, knocking down ETS2 did not influence the expression of another angiocrine factor, Jagged1 (Cao et al., 2014; Cao et al., 2016) in co-cultured HUVECs. This effect caused by ETS2 silencing in HUVECs was recapitulated by shRNA-mediated *Fgf4* knockdown in tumor cells (Figure 7E–G). Thus, tumor-derived FGF4 activates endothelial FGFR1 to induce ETS2-dependent IGF1 induction and IGFBP7 suppression in TECs (Figure 7H).

IGF1 and IGFBP7 compete to regulate chemoresistance in *Eμ-Myc* mice

To uncover the influence of divergent IGF1 and IGFBP7 function in TECs on mediating chemoresistance of primary tumors, *Myc*$^+$ mice were crossed with either *Igf1*$^{i\Delta EC/i\Delta EC}$ or *Igfbp7*$^{-/-}$ mice. Then, *Myc*$^+$ *Igf1*$^{i\Delta EC/i\Delta EC}$, *Myc*$^+$ *Igfbp7*$^{-/-}$ and control mice were subjected to doxorubicin treatment. EC-specific deletion of *Igf1* markedly prolonged mouse life span, decreased IGF1R phosphorylation, and elevated tumor cell apoptosis in *Myc*$^+$ mice after chemotherapy (Figure 8A–C). In contrast, genetic deletion of *Igfbp7* in chemotherapy-treated *Myc*$^+$ mice lowered animal survival, increased IGF1R activation, and reduced extent of apoptosis in *Myc*$^+$ LCs (Figure 8D–G, Figure S7). Hence, IGFBP7 secreted from host TECs represents an inhibitory checkpoint that prevents tumor cells from acquiring aggressive attributes, such as chemoresistance. Aberrant activation of FGF4-FGFR1-ETS2 axis in TECs abrogates this suppressor factor IGFBP7, upregulating IGF1 expression in TECs and stimulating expansion of aggressive IGF1R$^+$ TSCs (Figure 8H).

Discussion

In this report, we first identified a tumor-suppressive “checkpoint” function of IGFBP7/angiomodulin in TECs (Hooper et al., 2009; St Croix et al., 2000; van Beijnum et al., 2006). Inhibition of this checkpoint in TECs favors the outgrowth of chemoresistant TSCs in different organs. Tumor-derived FGF4 activates FGFR1 on TECs to induce expression of the transcription factor ETS2. By blocking expression of IGFBP7 and augmenting expression of IGF1, ETS2 hijacks TECs and subverts them to transform indolent tumors to chemoresistant and aggressive TSCs and increase tumor-mediated lethality of the host. This maladaptive activation of a tumor vascular niche is accompanied by reciprocal upregulation of the IGF1R-ligand IGF1 in TECs (Zhang et al., 2013). These results show that aberrant TSC characteristics need not to be hard-wired by cancer mutations nor completely cell autonomous. Rather key cancer phenotypes can be directed by cues from non-malignant but maladapted host TECs and the balance between IGF1, supporting aggressive features, and the checkpoint decision imposed on this signaling by TEC IGFBP7. Thus, our findings implicate an extrinsic ‘two-hit” process required for cancer stem cell-like features to manifest *in vivo*.

TECs deploy this chemoresistance-stimulating "two-hit” mechanism in multiple organs. The pro-tumorigenic function of TEC-derived IGF1 was apparent both *in vitro* using EC-tumor cell co-culture and *in vivo* using EC-specific genetic models. Although indirect contributions from other tumor niche components and cell types could also be involved, our data indicate that chemotherapy-induced expression of IGF1 by TECs contributes to the persistent aggressiveness of neighboring tumor cells. Conceivably, collaborating angiocrine signals elaborated from TECs could direct tumor phenotypes in combination by triggering potentially synergistic interactions between paracrine TEC-IGF1 and Notch-ligand (e.g., Jagged-1) activating IGF1R and juxtacrine Notch signaling in TSC (Cao et al., 2014; Lu et al., 2013). Notably, IGF1 induced subversion of vascular niche was found in TECs localized in lymph node, liver and lung. Thus, upregulation of IGF1 appears to be commonly involved in maladapted reprogramming of tumor-stimulating vascular niche in different organs and for multiple tumor types.

We identify a tumor-inhibitory “checkpoint” function of TECs in host. IGFBP7 is upregulated in TECs and inhibits IGF1R signaling in neighboring TSCs. Curiously, this IGFBP7-dependent brake was disrupted by chemotherapy, leading to the emergence of a chemoresistance-stimulating vascular niche composed of subverted TECs. It is plausible that chemotherapy triggered an injury response that altered the angiocrine activity of TECs. Indeed, we have found that angiocrine factors elaborated from tissue-specific ECs change during organ regeneration (Rafii et al., 2016). Early during tumor development, host ECs may express the "checkpoint" molecule, IGFBP7, to constrain cancer progression. But after injury they bypass this checkpoint possibly by displaying an angiocrine repertoire that forms a supportive microenvironment for aggressive $IGF1R^{+}$ TSCs. Indeed, such a stereotyped response to injury was seen in multiple tumor-harboring organs wherein chemotherapy suppressed IGFBP7 expression in TECs by a FGFR1-ETS2 mechanism, and simultaneously reinforced IGF1R signaling in TSCs by upregulating TEC IGF1 using this same mechanism. In this vein, induction of a chemoresistance-stimulating ligand, such as IGF1, and

suppression of checkpoint-like molecule could be a "hallmark" of a maladapted tumor vascular niche begetting cancer stem cells.

It is appreciated that chemotherapy selects for resistant tumors, and unless the treatment is able to completely eradicate cancer cells, recurrent tumors are typically resistant to retreatment using the agents to which they initially responded. Acquired mutations are often implicated in this process, but our findings suggest that cross-talk between the tumor cells and neighboring ECs subverts the tumor vascular niche and instigates the aggressive chemoresistant phenotype of IGF1R$^+$ TSCs. Chemotherapy induces aggressive tumor cells to upregulate FGF4 that then stimulates TEC FGFR1 and induces ETS2-dependent IGF1 upregulation and IGFBP7 suppression. It is conceivable that while chemotherapy eradicates the majority of tumor cells, chemoresistant perivascular IGF1R$^+$ TSCs co-opt neighboring ECs by inducing them to upregulate production of pro-tumorigenic angiocrine factors that reinforce chemoresistance and promote tumor recurrence and lethality. As such, we have unraveled a mechanism by which aggressive TSCs subjugate tumor-associated vascular niche.

Reversal of the maladapted function of the tumor vascular niche by selectively silencing tumorigenic or restoring niche-derived inhibitory cues is a promising therapeutic strategy. This approach would allow for modulating specific angiocrine factors instead of disrupting tumor vascular supply that paradoxically leads to rebound angiogenesis and tumor growth. This approach might be timely for designing effective cancer treatment because previous anti-angiogenic approaches aiming to abrogate tumor blood vessel growth have had limited success (Bogdanovich et al., 2016; Ebos et al., 2009; Paez-Ribes et al., 2009; Yasuma et al., 2016). Our data could potentially have clinical implications in which anti-IGF1R antibody along with IGFBP7 agonists could be employed in conjunction with chemotherapeutic agents to block IGF1R$^+$ TSCs (Wilky et al., 2015). As such, this study might help to design effective anti-chemoresistance strategy by disrupting crosstalk between cancer stem cells and their aberrantly activated vascular niche.

Experimental procedures

Animals

Generation of mice with deletion of *Igfbp7/angiomodulin* was previously described (Hooper et al., 2009). DN-03 anaplastic large cell lymphoma (ALCL) PDTX Mouse model was generated as previously described (Cheng et al., 2012). *Igfbp7*$^{-/-}$ mice were generated with proper mendelian ratio without salient embryonic lethality. *Eμ-Myc* mice were crossed with *Igfbp7*$^{-/-}$ *mice* to generate *Myc*$^+$*Igfbp7*$^{-/-}$ or *Myc*$^+$*Igfbp7*$^{+/+}$ mice. Floxed *Fgfr1* or *Igf1* (Jax No. 016831) mice were crossed with VE-cadherin-Cre^{ERT2} (*cdh5-PAC-Cre*^{ERT2}) transgenic mice (kindly provided by Dr. Ralf H. Adams), and resultant VE-cadherin-Cre^{ERT2}*Fgfr1*$^{loxp/loxp}$ or VE-cadherin-Cre^{ERT2}*Igf1*$^{loxp/loxp}$ mice were treated with tamoxifen to induce EC-specific deletion of *Fgfr1* or *Igf1* in the adult mice. Briefly, mice were treated with tamoxifen at a dose of 150 mg/kg i.p. for 6 days interrupted for 3 days after the third dose. Deletion of target genes in tumor ECs was corroborated by quantitative PCR and immunoblot analysis. All animal experiments were approved by Institutional Animal Care and Use Committee (IACUC) at Weill Cornell Medicine.

In vitro serum/cytokine free co-culture of tumor cells and ECs

HUVECs were transduced with the adenoviral E4ORF1 gene, which activates low level of Akt signaling pathway and endows ECs with the ability of surviving in serum/cytokine free environment (Cao et al., 2014; Seandel et al., 2008). E4-HUVECs establish a resilient, responsive and unbiased generic vascular niche model to maintain tumor cell survival in serum/growth factor free environment without distractive effects from serum supplementation. E4-HUVECs are referred here for simplicity as ECs. shRNA-mediated gene knockdown was utilized to selectively knock down IGF1, FGFR1 in ECs and FGF4 and IGF1R in tumor cells. Lentiviruses were generated by co-transfecting 15 μg of shuttle lentiviral vector containing specific gene-targeted shRNA or scrambled shRNA (Cao et al., 2014). For serum/growth factor-free co-culture experiments, Srb-transduced ECs or ECs with genetic silencing of IGF1 and FGFR1 were cultured in 6 well plate at $1x10^5$ cells/well. Tumor cell clones were seeded on top of the monolayer formed by ECs at 1000 cells/well. After 8 or 12 days after co-culture, the number of tumor cell was quantified by flow cytometric analysis.

Assay for chemoresistance of tumor cells

To measure chemoresistance *in vitro*, LCs and HCCs were derived from *Eμ-Myc* and *Lap-Myc* mice, as previously described (Cao et al., 2014; Cao et al., 2011; Shachaf et al., 2004). The cells were treated with 0.005–0.01 μg/ml doxorubicin. The percentage of dead cells was distinguished with 0.4% trypan blue solution. Cell lines exhibiting high chemoresistance were named as line 1 to line 5. Cell line manifesting the lowest tolerance to doxorubicin was named as line 6.

Two million LCs, HCCs, and LLCs were transplanted to mice deficient of endothelial *Igf1* (*Igf1*$^{i\Delta EC/i\Delta EC}$), *Fgfr1* (*Fgf1*$^{i\Delta EC/i\Delta EC}$) and *Igfbp7* (*Igfbp7*$^{-/-}$). To test the response in different vascular beds, LCs and HCCs were injected into the liver vasculature by a liver seeding model (Ding et al., 2011), and LCs and LLCs were administered via jugular vein. To measure chemoresistance *in vivo*, mice were treated with 10 mg/kg doxorubicin, 5-FU, or 5 mg/kg cisplatin once a week at day 7 after transplantation. Effect of doxorubicin, 5-FU and cisplatin was analyzed in recipient mice, including tumor load and animal survival.

To test the therapeutic effect of recombinant IGFBP7 (R&D) or IGF1R neutralizing antibody (Santa Cruz, clone 1H7), 10 ug IGFBP7 was injected into the tumor carrying mice every three days at day 7 after tumor transplantation. Meanwhile, 20 μg antibody and isotype IgG was also administered every week to determine the effect on mouse survival and tumor load.

To test cell death and proliferation in lymphoma, mice were sacrificed and cryopreserved sections were incubated with the mixture of terminal deoxynucleotidyl transferase, nucleotide and reaction buffer as indicated by TUNEL *In Situ* Cell Death Detection Kit (Roche). Tumor load was calculated by percent of tumor area, and tumor area was identified by neoplastic morphology distinct from normal tissue. Images were captured with AxioVert LSM710 confocal microscope (Zeiss).

Methylcellulose colony assay

LCs isolated from *Eμ-Myc* mice were suspended in methylcellulose medium (StemCell Technologies) at the concentration of 500 cells/ml as previously described. The mixture was seeded in 6 well plate and incubated in 37°C for 5 days. The colony number was counted.

Cell isolation

Mouse endothelial cells and tumor cells were isolated from tumor mass by flow sorting as previously described (Cao et al., 2016; Nolan et al., 2013; Rafii et al., 2015). TECs and tumor cells were identified by rat anti-mouse CD31 (clone Mec13.3) and VE-cadherin (clone Bv13) antibodies (for TECs) and mCherry fluorescent protein (for tumor cells). Tumor tissue was digested in a digestion cocktail solution containing 2 mg/ml collogenase A and 1 mg/ml Dispase (Roche Life Science) in Hanks' Balanced Salted Solution (HBSS). Perfused mouse tumor tissues were carefully removed and dissected in RPMI1640 medium (Life Technologies), gently minced, and disrupted by passing through a 18 Gauge syringe. After filtration, released cells were incubated with 1 μg/ml fluorescently labeled rat-anti mouse VE-cadherin and CD31 antibodies for flow sorting. Fluorescent antibody-stained cells were collected using a flow sorter, and isolated TECs or tumor cells were directly subjected to subsequent analyses, unless specified as cultivated cells. Phosphorylated Akt and IGF1R was analyzed by Western blot (Cell Signaling, Cat No. 4060 and 4568). All presented lanes in one Western blot strip were derived and adjusted equally from the same corresponding blot. The flow cytometry data were collected by LSRII flow cytometer (BD Biosciences) and analyzed by as previously described (Cao et al., 2014).

Immunostaining analysis of mouse tissue

Mouse tissue was fixed with 4% PFA, cryopreserved, and processed with Leica CM3050 S to 8 μm slice. The sections were blocked with 5% donkey serum/0.3% Triton X-100 and incubated with primary antibody against VE-Cadherin (R&D Systems), IGF1R and phosphor-IGF1R (Cell Signaling Technology), and Ki67 (DAKO). Sections were then incubated with fluorescence-labeled secondary antibody (Jackson ImmunoResearch), followed by counterstaining with DAPI (Invitrogen). Images were captured with AxioVert LSM710 confocal microscope (Zeiss).

Statistical analysis of data

All data were presented as the mean ± standard error of mean (SEM) of at least three separate experiments. Analysis of variance (ANOVA) was used to compare groups in Kaplan Meier graphs. Statistical significance was set at $p < 0.05$.

Supplementary Material

Refer to Web version on PubMed Central for supplementary material.

Acknowledgments

We are indebted to Dr. Michael Ginsberg at Angiocrine Bioscience for supplying mouse endothelial cells and Drs. Dean W. Felsher and Stephanie C. Casey at Stanford University for kindly providing mouse HCC cells. We are grateful to Dr. Ralf Adams at Max Planck Institute and Dr. Michael Simons at Yale University for generously

sharing Chd5(PAC)-Cre^{ERT2} and floxed *Fgfr1* mice. We also thank Mr. Deebly Chavez for his assist with animal procedure. Z.C. was supported by Druckenmiller Fellowship from the New York Stem Cell Foundation. This work was also supported by a National Scientist Development Grant from the American Heart Association (12SDG1213004) and National Heart, Lung, and Blood Institute R01HL130826-01. S.R. is supported by the Ansary Stem Cell Institute, the Empire State Stem Cell Board and New York State Department of Health grants (C024180, C026438, C026878, C028117), NIH R01HL097797 and R01HL119872. S.R. is the founder and non-paid consultant to the Angiocrine Bioscience, New York, N.Y. GI is supported by the by Italian Association for Cancer Research (AIRC) (5x1000 No. 10007).

References

Beck B, Driessens G, Goossens S, Youssef KK, Kuchnio A, Caauwe A, Sotiropoulou PA, Loges S, Lapouge G, Candi A, et al. A vascular niche and a VEGF-Nrp1 loop regulate the initiation and stemness of skin tumours. Nature. 2011; 478:399–403. [PubMed: 22012397]

Bergers G, Hanahan D. Modes of resistance to anti-angiogenic therapy. Nat Rev Cancer. 2008; 8:592–603. [PubMed: 18650835]

Bogdanovich S, Kim Y, Mizutani T, Yasuma R, Tudisco L, Cicatiello V, Bastos–Carvalho A, Kerur N, Hirano Y, Baffi JZ, et al. Human IgG1 antibodies suppress angiogenesis in a target-independent manner. Signal transduction and targeted therapy. 2016 (1. pii: 15001. Epub 2016 Jan 28).

Bono F, De Smet F, Herbert C, De Bock K, Georgiadou M, Fons P, Tjwa M, Alcouffe C, Ny A, Bianciotto M, et al. Inhibition of tumor angiogenesis and growth by a small-molecule multi-FGF receptor blocker with allosteric properties. Cancer cell. 2013; 23:477–488. [PubMed: 23597562]

Calabrese C, Poppleton H, Kocak M, Hogg TL, Fuller C, Hamner B, Oh EY, Gaber MW, Finklestein D, Allen M, et al. A perivascular niche for brain tumor stem cells. Cancer Cell. 2007; 11:69–82. [PubMed: 17222791]

Cao Z, Ding BS, Guo P, Lee SB, Butler JM, Casey SC, Simons M, Tam W, Felsher DW, Shido K, et al. Angiocrine factors deployed by tumor vascular niche induce B cell lymphoma invasiveness and chemoresistance. Cancer cell. 2014; 25:350–365. [PubMed: 24651014]

Cao Z, Fan-Minogue H, Bellovin DI, Yevtodiyenko A, Arzeno J, Yang Q, Gambhir SS, Felsher DW. MYC phosphorylation, activation, and tumorigenic potential in hepatocellular carcinoma are regulated by HMG-CoA reductase. Cancer research. 2011; 71:2286–2297. [PubMed: 21262914]

Cao Z, Lis R, Ginsberg M, Chavez D, Shido K, Rabbany SY, Fong GH, Sakmar TP, Rafii S, Ding BS. Targeting of the pulmonary capillary vascular niche promotes lung alveolar repair and ameliorates fibrosis. Nature medicine. 2016; 22:154–162.

Carmeliet P, Jain RK. Molecular mechanisms and clinical applications of angiogenesis. Nature. 2011; 473:298–307. [PubMed: 21593862]

Chao MP, Alizadeh AA, Tang C, Myklebust JH, Varghese B, Gill S, Jan M, Cha AC, Chan CK, Tan BT, et al. Anti-CD47 antibody synergizes with rituximab to promote phagocytosis and eradicate non-Hodgkin lymphoma. Cell. 2010; 142:699–713. [PubMed: 20813259]

Chen D, Siddiq A, Emdad L, Rajasekaran D, Gredler R, Shen XN, Santhekadur PK, Srivastava J, Robertson CL, Dmitriev I, et al. Insulin-like growth factor-binding protein-7 (IGFBP7): a promising gene therapeutic for hepatocellular carcinoma (HCC). Molecular therapy : the journal of the American Society of Gene Therapy. 2013; 21:758–766.

Cheng M, Quail MR, Gingrich DE, Ott GR, Lu L, Wan W, Albom MS, Angeles TS, Aimone LD, Cristofani F, et al. CEP-28122, a highly potent and selective orally active inhibitor of anaplastic lymphoma kinase with antitumor activity in experimental models of human cancers. Mol Cancer Ther. 2012; 11:670–679. [PubMed: 22203728]

Ding BS, Cao Z, Lis R, Nolan DJ, Guo P, Simons M, Penfold ME, Shido K, Rabbany SY, Rafii S. Divergent angiocrine signals from vascular niche balance liver regeneration and fibrosis. Nature. 2014; 505:97–102. [PubMed: 24256728]

Ding BS, Nolan DJ, Butler JM, James D, Babazadeh AO, Rosenwaks Z, Mittal V, Kobayashi H, Shido K, Lyden D, et al. Inductive angiocrine signals from sinusoidal endothelium are required for liver regeneration. Nature. 2010; 468:310–315. [PubMed: 21068842]

Ding BS, Nolan DJ, Guo P, Babazadeh AO, Cao Z, Rosenwaks Z, Crystal RG, Simons M, Sato TN, Worgall S, et al. Endothelial-derived angiocrine signals induce and sustain regenerative lung alveolarization. Cell. 2011; 147:539–553. [PubMed: 22036563]

Ding L, Saunders TL, Enikolopov G, Morrison SJ. Endothelial and perivascular cells maintain haematopoietic stem cells. Nature. 2012; 481:457–462. [PubMed: 22281595]

Ebos JM, Lee CR, Cruz-Munoz W, Bjarnason GA, Christensen JG, Kerbel RS. Accelerated metastasis after short-term treatment with a potent inhibitor of tumor angiogenesis. Cancer Cell. 2009; 15:232–239. [PubMed: 19249681]

Evdokimova V, Tognon CE, Benatar T, Yang W, Krutikov K, Pollak M, Sorensen PH, Seth A. IGFBP7 binds to the IGF-1 receptor and blocks its activation by insulin-like growth factors. Sci Signal. 2012; 5:ra92. [PubMed: 23250396]

Franses JW, Baker AB, Chitalia VC, Edelman ER. Stromal endothelial cells directly influence cancer progression. Science translational medicine. 2014; 3:66ra65.

Ghajar CM, Peinado H, Mori H, Matei IR, Evason KJ, Brazier H, Almeida D, Koller A, Hajjar KA, Stainier DY, et al. The perivascular niche regulates breast tumour dormancy. Nat Cell Biol. 2013; 15:807–817. [PubMed: 23728425]

Gilbert LA, Hemann MT. DNA damage-mediated induction of a chemoresistant niche. Cell. 2010; 143:355–366. [PubMed: 21029859]

Hanahan D, Coussens LM. Accessories to the crime: functions of cells recruited to the tumor microenvironment. Cancer Cell. 2012; 21:309–322. [PubMed: 22439926]

Hayakawa Y, Ariyama H, Stancikova J, Sakitani K, Asfaha S, Renz BW, Dubeykovskaya ZA, Shibata W, Wang H, Westphalen CB, et al. Mist1 Expressing Gastric Stem Cells Maintain the Normal and Neoplastic Gastric Epithelium and Are Supported by a Perivascular Stem Cell Niche. Cancer cell. 2015; 28:800–814. [PubMed: 26585400]

Hoey T, Yen WC, Axelrod F, Basi J, Donigian L, Dylla S, Fitch-Bruhns M, Lazetic S, Park IK, Sato A, et al. DLL4 blockade inhibits tumor growth and reduces tumor-initiating cell frequency. Cell Stem Cell. 2009; 5:168–177. [PubMed: 19664991]

Hooper AT, Shmelkov SV, Gupta S, Milde T, Bambino K, Gillen K, Goetz M, Chavala S, Baljevic M, Murphy AJ, et al. Angiomodulin is a specific marker of vasculature and regulates vascular endothelial growth factor-A-dependent neoangiogenesis. Circ Res. 2009; 105:201–208. [PubMed: 19542015]

Hu J, Srivastava K, Wieland M, Runge A, Mogler C, Besemfelder E, Terhardt D, Vogel MJ, Cao L, Korn C, et al. Endothelial cell-derived angiopoietin-2 controls liver regeneration as a spatiotemporal rheostat. Science (New York, NY. 2014; 343:416–419.

Lu J, Ye X, Fan F, Xia L, Bhattacharya R, Bellister S, Tozzi F, Sceusi E, Zhou Y, Tachibana I, et al. Endothelial Cells Promote the Colorectal Cancer Stem Cell Phenotype through a Soluble Form of Jagged-1. Cancer Cell. 2013; 23:171–185. [PubMed: 23375636]

Magee JA, Piskounova E, Morrison SJ. Cancer stem cells: impact, heterogeneity, and uncertainty. Cancer cell. 2012; 21:283–296. [PubMed: 22439924]

Medyouf H, Gusscott S, Wang H, Tseng JC, Wai C, Nemirovsky O, Trumpp A, Pflumio F, Carboni J, Gottardis M, et al. High-level IGF1R expression is required for leukemia-initiating cell activity in T-ALL and is supported by Notch signaling. J Exp Med. 2011; 208:1809–1822. [PubMed: 21807868]

Nakasone ES, Askautrud HA, Kees T, Park JH, Plaks V, Ewald AJ, Fein M, Rasch MG, Tan YX, Qiu J, et al. Imaging tumor-stroma interactions during chemotherapy reveals contributions of the microenvironment to resistance. Cancer Cell. 2012; 21:488–503. [PubMed: 22516258]

Nolan DJ, Ginsberg M, Israely E, Palikuqi B, Poulos MG, James D, Ding BS, Schachterle W, Liu Y, Rosenwaks Z, et al. Molecular signatures of tissue-specific microvascular endothelial cell heterogeneity in organ maintenance and regeneration. Dev Cell. 2013; 26:204–219. [PubMed: 23871589]

Paez-Ribes M, Allen E, Hudock J, Takeda T, Okuyama H, Vinals F, Inoue M, Bergers G, Hanahan D, Casanovas O. Antiangiogenic therapy elicits malignant progression of tumors to increased local invasion and distant metastasis. Cancer Cell. 2009; 15:220–231. [PubMed: 19249680]

Passegue E, Rafii S, Herlyn M. Cancer stem cells are everywhere. Nat Med. 2009; 15:23. [PubMed: 19129778]

Phan VT, Wu X, Cheng JH, Sheng RX, Chung AS, Zhuang G, Tran C, Song Q, Kowanetz M, Sambrone A, et al. Oncogenic RAS pathway activation promotes resistance to anti-VEGF therapy

through G-CSF-induced neutrophil recruitment. Proceedings of the National Academy of Sciences of the United States of America. 2013; 110:6079–6084. [PubMed: 23530240]

Pitt LA, Tikhonova AN, Hu H, Trimarchi T, King B, Gong Y, Sanchez-Martin M, Tsirigos A, Littman DR, Ferrando AA, et al. CXCL12-Producing Vascular Endothelial Niches Control Acute T Cell Leukemia Maintenance. Cancer Cell. 2014; 27:755–768.

Plaks V, Kong N, Werb Z. The cancer stem cell niche: how essential is the niche in regulating stemness of tumor cells? Cell stem cell. 2015; 16:225–238. [PubMed: 25748930]

Quintana E, Shackleton M, Sabel MS, Fullen DR, Johnson TM, Morrison SJ. Efficient tumour formation by single human melanoma cells. Nature. 2008; 456:593–598. [PubMed: 19052619]

Rafii S, Butler JM, Ding BS. Angiocrine functions of organ-specific endothelial cells. Nature. 2016; 529:316–325. [PubMed: 26791722]

Rafii S, Cao Z, Lis R, Siempos II, Chavez D, Shido K, Rabbany SY, Ding BS. Platelet-derived SDF-1 primes the pulmonary capillary vascular niche to drive lung alveolar regeneration. Nature cell biology. 2015; 17:123–136. [PubMed: 25621952]

Schepers K, Campbell TB, Passegue E. Normal and leukemic stem cell niches: insights and therapeutic opportunities. Cell stem cell. 2015; 16:254–267. [PubMed: 25748932]

Schmidt T, Kharabi Masouleh B, Loges S, Cauwenberghs S, Fraisl P, Maes C, Jonckx B, De Keersmaecker K, Kleppe M, Tjwa M, et al. Loss or inhibition of stromal-derived PlGF prolongs survival of mice with imatinib-resistant Bcr-Abl1(+) leukemia. Cancer Cell. 2011; 19:740–753. [PubMed: 21665148]

Seandel M, Butler JM, Kobayashi H, Hooper AT, White IA, Zhang F, Vertes EL, Kobayashi M, Zhang Y, Shmelkov SV, et al. Generation of a functional and durable vascular niche by the adenoviral E4ORF1 gene. Proceedings of the National Academy of Sciences of the United States of America. 2008; 105:19288–19293. [PubMed: 19036927]

Shachaf CM, Kopelman AM, Arvanitis C, Karlsson A, Beer S, Mandl S, Bachmann MH, Borowsky AD, Ruebner B, Cardiff RD, et al. MYC inactivation uncovers pluripotent differentiation and tumour dormancy in hepatocellular cancer. Nature. 2004; 431:1112–1117. [PubMed: 15475948]

St Croix B, Rago C, Velculescu V, Traverso G, Romans KE, Montgomery E, Lal A, Riggins GJ, Lengauer C, Vogelstein B, et al. Genes expressed in human tumor endothelium. Science. 2000; 289:1197–1202. [PubMed: 10947988]

Tavora B, Reynolds LE, Batista S, Demircioglu F, Fernandez I, Lechertier T, Lees DM, Wong PP, Alexopoulou A, Elia G, et al. Endothelial-cell FAK targeting sensitizes tumours to DNA-damaging therapy. Nature. 2014; 514:112–116. [PubMed: 25079333]

Trimarchi T, Bilal E, Ntziachristos P, Fabbri G, Dalla-Favera R, Tsirigos A, Aifantis I. Genome-wide mapping and characterization of Notch-regulated long noncoding RNAs in acute leukemia. Cell. 2014; 158:593–606. [PubMed: 25083870]

van Beijnum JR, Dings RP, van der Linden E, Zwaans BM, Ramaekers FC, Mayo KH, Griffioen AW. Gene expression of tumor angiogenesis dissected: specific targeting of colon cancer angiogenic vasculature. Blood. 2006; 108:2339–2348. [PubMed: 16794251]

Verhagen HJ, de Leeuw DC, Roemer MG, Denkers F, Pouwels W, Rutten A, Celie PH, Ossenkoppele GJ, Schuurhuis GJ, Smit L. IGFBP7 induces apoptosis of acute myeloid leukemia cells and synergizes with chemotherapy in suppression of leukemia cell survival. Cell death & disease. 2014; 5:e1300. [PubMed: 24967962]

Wajapeyee N, Serra RW, Zhu X, Mahalingam M, Green MR. Oncogenic BRAF induces senescence and apoptosis through pathways mediated by the secreted protein IGFBP7. Cell. 2008; 132:363–374. [PubMed: 18267069]

Weis SM, Cheresh DA. Tumor angiogenesis: molecular pathways and therapeutic targets. Nat Med. 2011; 17:1359–1370. [PubMed: 22064426]

Wilky BA, Rudek MA, Ahmed S, Laheru DA, Cosgrove D, Donehower RC, Nelkin B, Ball D, Doyle LA, Chen H, et al. A phase I trial of vertical inhibition of IGF signalling using cixutumumab, an anti-IGF-1R antibody, and selumetinib, an MEK 1/2 inhibitor, in advanced solid tumours. British journal of cancer. 2015; 112:24–31. [PubMed: 25268371]

Yasuma R, Cicatiello V, Mizutani T, Tudisco L, Kim Y, Tarallo V, Bogdanovich S, Hirano Y, Kerur N, Li S, et al. Intravenous immune globulin suppresses angiogenesis in mice and humans. Signal transduction and targeted therapy. 2016 (1. pii: 15002. Epub 2016 Jan 28).

Zhang XH, Jin X, Malladi S, Zou Y, Wen YH, Brogi E, Smid M, Foekens JA, Massague J. Selection of bone metastasis seeds by mesenchymal signals in the primary tumor stroma. Cell. 2013; 154:1060–1073. [PubMed: 23993096]

Significance

Stem cell-like features of tumors are thought to be cell-autonomous. Our data challenge this hypothesis and support an alternative model wherein maladapted tumor-associated-vascular endothelial cells (TECs) constitute a subverted vascular niche that confers stem cell-like activity to indolent tumor cells. Abnormal activation of FGFR1-ETS2 pathway in TECs enforces aggressiveness and chemoresistance in multiple mouse and human tumor models. Subversion of TECs to form this pro-tumorigenic vascular niche relies on a "two-hit" mechanism: downregulation of tumor suppressor/checkpoint IGFBP7 and upregulation of IGF1. Imbalanced IGFBP7 and IGF1 angiocrine expression in TECs induces generation and engraftment of cancer stem cell-like cells. Thus, our study defines a molecular hub that coopts TECs to form a tumor vascular-niche inducing a cancer stem cell phenotype.

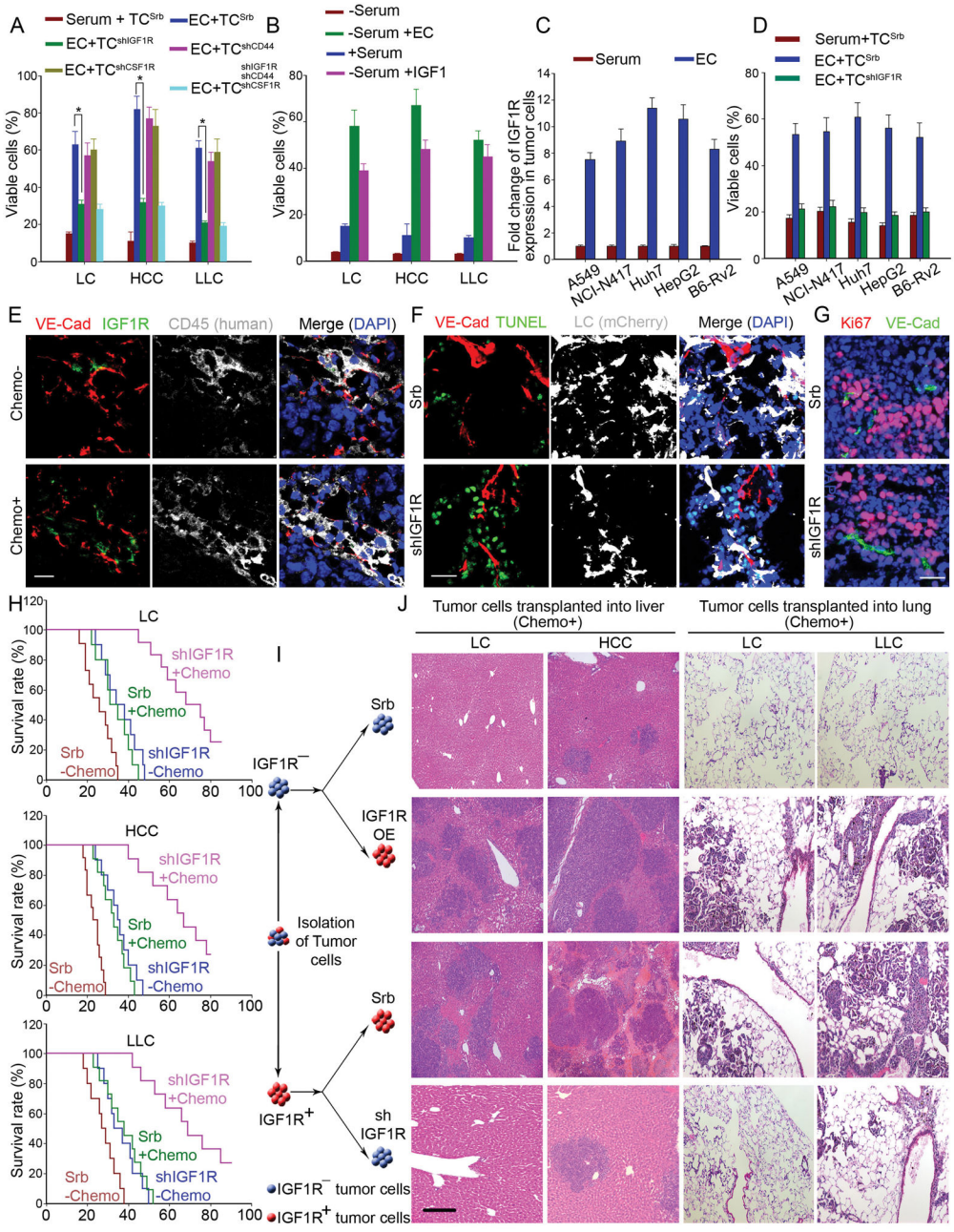

Figure 1. Endothelial cells (ECs) induce IGF1R in tumor cells to confer resistance to chemotherapeutic agent

(A) Chemoresistance of tumor cells after co-culturing with E4ORF1 transduced primary human umbilical cord vein ECs (HUVECs) at serum-free and growth factor free condition. In *Myc*$^{+}$-induced lymphoma cells (LCs), hepatocellular carcinoma cells (HCCs), and Lewis lung carcinoma cells (LLCs), shRNA was used to silence the expression of IGF1R ($TC^{shIGF1R}$), CD44 (TC^{shCD44}), CSF1R ($TC^{shCSF1R}$). Scrambled shRNA transduced tumor cells (TC^{Srb}) were used as control. Tumor cells were cultured in serum-containing medium (Serum + TC) or co-cultured with ECs in serum-free condition (EC + TC) and treated with doxorubicin or vehicle. Number of viable tumor cells after doxorubicin treatment was

compared to that of vehicle-treated cells (percentage of viable cells); n = 6 per group. Data are represented as mean ± standard error mean (S.E.M) throughout the manuscript.

(**B**) Tolerance of tumor cells to doxorubicin after supplementation of IGF1 in serum-free culture condition ; n = 5–6 per group.

(**C**) Induction of IGF1R in tested tumor cell lines after EC co-culture. Tumor cells were incubated with HUVECs, and expression of IGF1R was quantified; n = 7 per group.

(**D**) Tolerance of indicated tumor cell lines to doxorubicin treatment; n = 6 per group.

(E) Expression of IGF1R in human patient-derived tumor xenograft (PDTX) model. Human patient-derived lymphoma cells were engrafted into immunodeficient mice as described (Cheng et al., 2012). Immunostaining of IGF1R was performed in lymphoma tissue from PDTX mice that received control or CHOP chemotherapy regimen, cyclophosphamide, hydroxydaunorubicin, oncovin, and prednisolone. Note the proximity between $IGF1R^+$ LCs expressing human CD45 with VE-$cadherin^+$ tumor-associated ECs (TECs) in the PDTX mice. Scale bar = 50 μm in Figure 1.

(F–G) Cell apoptosis and proliferation in isolated $IGF1R^+$ LCs transplanted into wild-type (WT) mice. LCs with IGF1R knockdown (shIGF1R) were transplanted to recipient mice and compared with LCs transduced with scrambled sequence (Srb). Cell death after chemotherapy was examined by TUNEL staining and proliferation was measured by Ki67 staining in lymphoma cryosections. Of note, there was a higher extent of apoptosis (TUNEL) in shIGF1R-transduced LCs. In contrast, there was no significant difference in cell proliferation between different groups, as evidenced by Ki67 staining.

(**H**) Survival curve of different groups of tumor cells after transplantation into mice with (+Chemo) or without (-Chemo) doxorubicin treatment. Mice were intraperitoneally (i.p.) injected with LCs, HCCs, or intravenously (i.v.) injected with LLCs. Tumor cells were transduced with shIGF1R or Srb; $p < 0.05$ between shIGF1R+Chemo group and all other groups; n = 10–12 mice per group.

(**I–J**) Expression of IGF1R and *in vivo* chemoresistance in transplanted tumor cells. IGF1R function was tested by gene overexpression (OE) or shRNA (shIGF1R) (I). LCs and HCCs were transplanted to the liver of mice by intrasplenic injection, and LCs and LLCs were transplanted into the mouse lungs via intravenous infusion. Mice were treated with doxorubicin, and hepatic and pulmonary tumor load in different groups were then analyzed (J).

See also Figure S1.

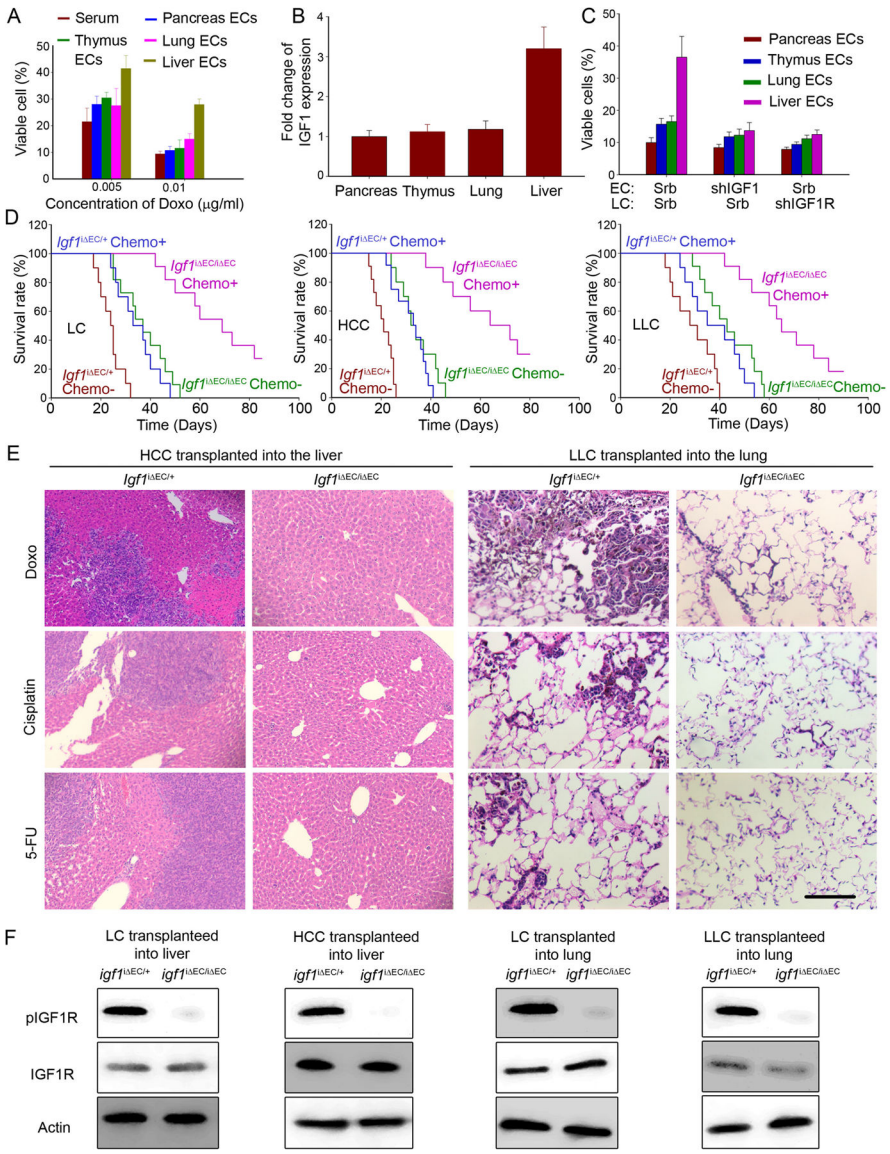

Figure 2. Insulin-like growth factor-1 (IGF1) supplied by tumor-associated ECs (TECs) stimulates chemoresistance in IGF1R$^+$ tumor propagating cells (TSCs)

(**A**) Resistance to doxorubicin treatment in LCs after co-culture with mouse liver, thymus, lung, and pancreas ECs. Number of viable lymphoma cell number after doxorubicin treatment was compared with LCs treated with vehicle after one week co-culture with ECs; n = 6 per group.

(**B, C**) IGF1 from liver ECs endows IGF1R-dependent resistance against doxorubicin. IGF1 expressed by liver ECs augmented expansion of chemoresistant IGF1R$^+$ LCs than did pancreas, thymus and lung ECs. shRNA knockdown of IGF1 (shIGF1) in liver ECs attenuated expansion of LCs to a comparable level caused by pancreas, thymus and lung ECs, or knocking down IGF1R (shIGF1R) in LCs (C); n = 5 per group.

(**D**) Survival curve of mice with endothelial cell (EC)-specific deletion of *Igf1* (*Igf1*$^{i\Delta EC/i\Delta EC}$) following tumor cell inoculation and doxorubicin treatment. LCs, HCCs

were transplanted to *Igf1*$^{i\Delta EC/i\Delta EC}$ or control (*Igf1*$^{i\Delta EC/+}$) mice by i.p. injection, and LLCs were i.v. injected to recipient mice. Survival of recipient mice was monitored upon doxorubicin (Chemo+) or vehicle (Chemo-) treatment. *Igf1*$^{i\Delta EC/i\Delta EC}$ mice were generated by crossing floxed *Igf1* mice with mice harboring EC-specific VE-cadherin-Cre^{ERT2} (cdh5(PAC)-Cre^{ERT2}); $p < 0.05$ between *Igf1*$^{i\Delta EC/i\Delta EC}$+Chemo group and all other groups; n = 11–13 mice per group.

(**E–F**) Influence of endothelial cell supplied IGF1 on chemoresistance of tumor cells transplanted in different vascular beds. LCs and HCCs were transplanted into the liver of *Igf1*$^{i\Delta EC/i\Delta EC}$ or control *Igf1*$^{i\Delta EC/+}$ mice by intrasplenic injection, LCs and LLCs were also i.v. transplanted into the lung of *Igf1*$^{i\Delta EC/i\Delta EC}$ or control mice. After mice were treated with doxorubicin, 5-fluorouracil (5-FU), and cisplatin, hepatic and pulmonary tumor load were analyzed (E), and level of total and activated (phosphorylated) IGF1R in isolated tumor cells was tested by Western blot (F). Scale bar = 50 μm; n = 8–9 mice per group.

See also Figure S2.

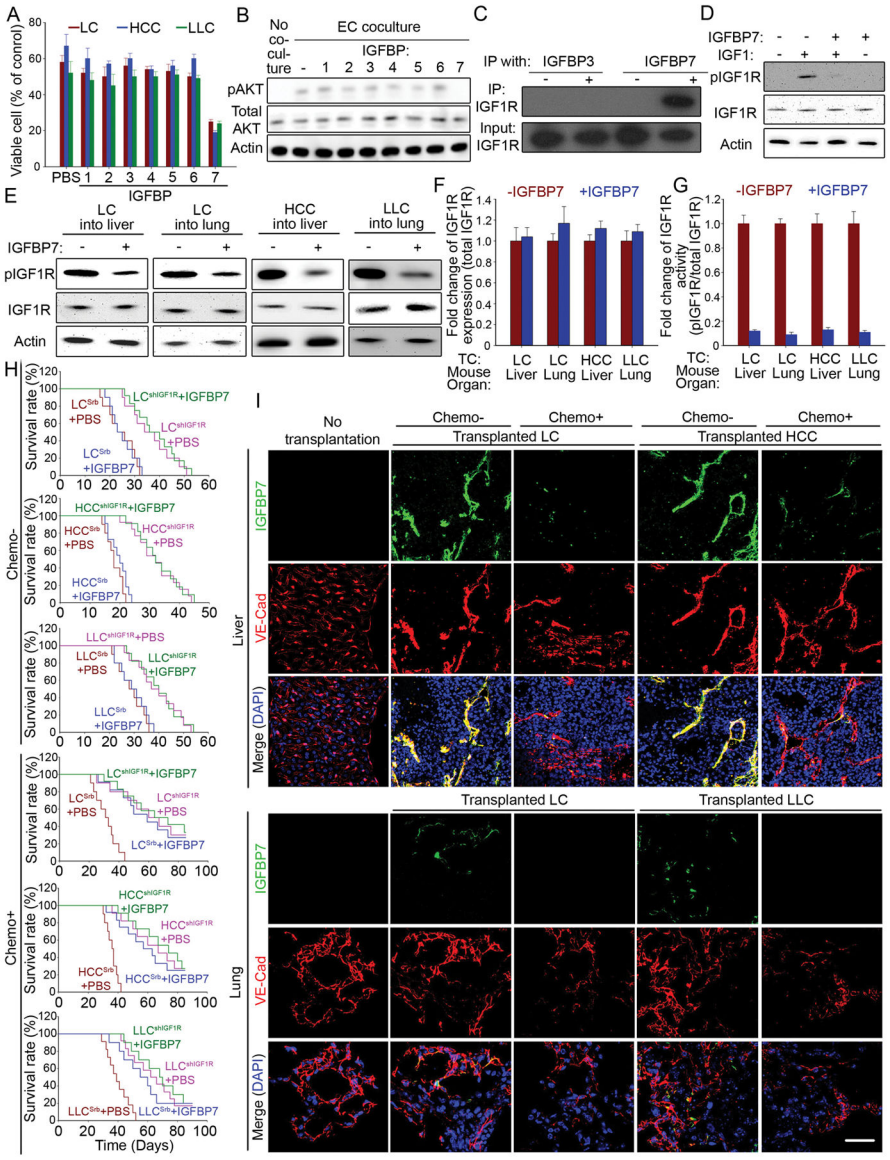

Figure 3. TECs express IGF1R antagonist IGFBP7 to suppress IGF1R-dependent chemoresistance in TSCs

(**A–B**) Efficacy of insulin growth factor binding protein 7 (IGFBP7/angiomodulin) in inhibiting IGF1R-dependent chemoresistance and Akt activation in LCs; n = 8 per group.

(**C–D**) Immunoprecipitation experiment with recombinant IGFBP7 and LC lysates showed that IGFBP7 associates with IGF1R in LCs (C) and blocks IGF1-mediated IGF1R activation (D). In contrast, IGFBP3 did not bind to IGF1R.

(**E–G**) IGF1R expression and activation/phosphorylation (pIGF1R) in transplanted tumor cells after treatment of IGFBP7. LCs, HCCs, and LLCs were isolated and protein levels of total and phosphorylated IGF1R were assayed by Western blot (E) and quantified (F, G).

(**H**) Effect of IGFBP7 on chemoresistance in transplanted tumor cells. IGF1R was silenced in tumor cells by shRNA (shIGF1R), and IGF1R^{+} tumor cells were i.p. or i.v. transplanted into WT mice. Recipient mice were treated with IGFBP7 or PBS with (top three "Chemo-"

graphs) or without (bottom three "Chemo+" graphs) doxorubicin treatment. Mouse survival was monitored; n = 10–14 mice per group.

(**I**) IGFBP7 was specifically induced in ECs upon tumor cell transplantation, and this expression was markedly lower in ECs of chemoresistant tumor that outgrew after doxorubicin treatment. Scale bar = 50 μm.

See also Figure S3.

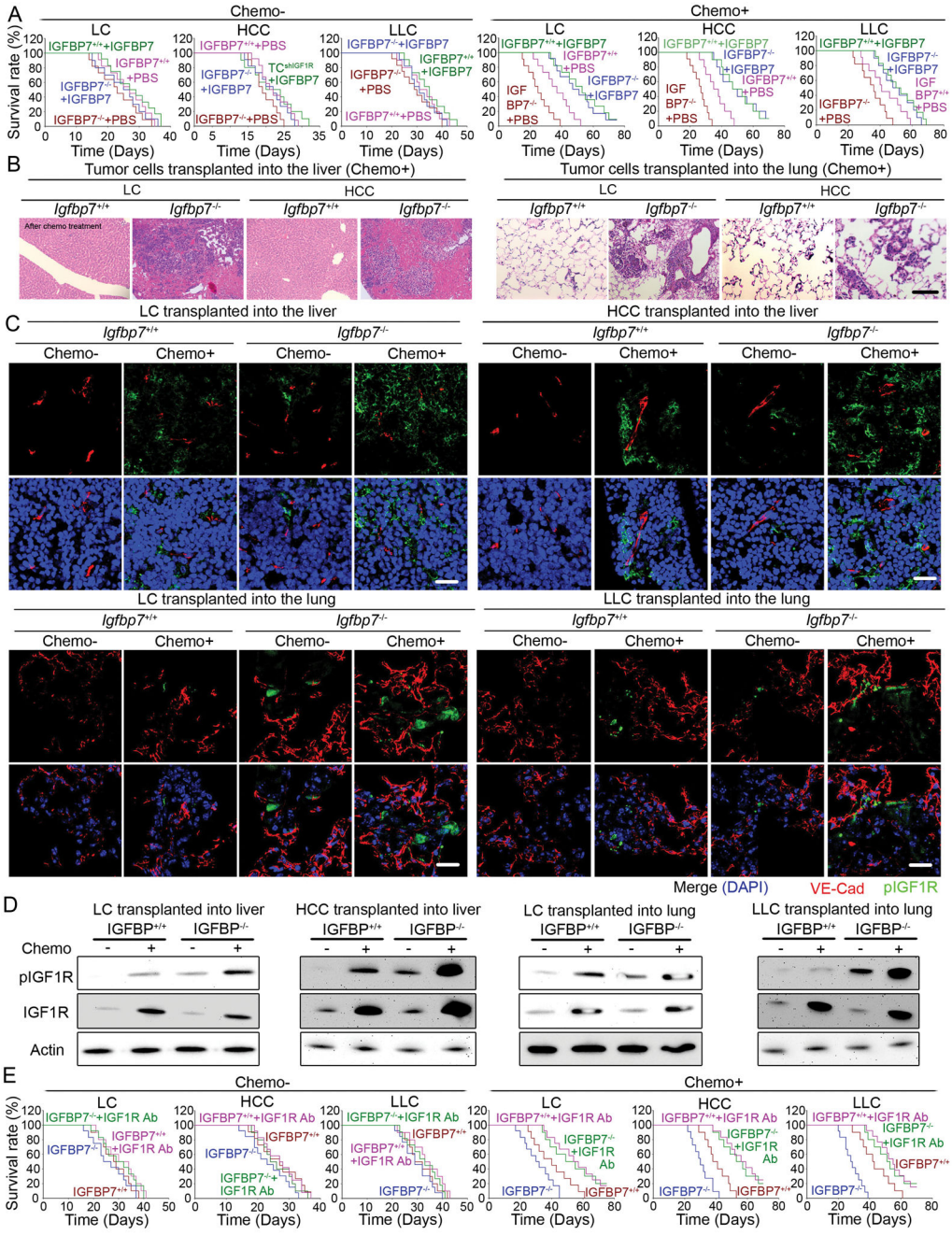

Figure 4. Chemoresistance of tumor cells transplanted into mice deficient of *Igfbp7* (*Igfbp7*$^{-/-}$)

(A) Effect of endothelial IGFBP7 on IGF1R-dependent chemoresistance in tumor cells. Tumor cells were i.p. or i.v. transplanted into *Igfbp7*$^{-/-}$ or control *Igfbp7*$^{+/+}$ mice. Recipient mice were treated with recombinant IGFBP7 and doxorubicin. n = 10–15 mice per group. (**B–C**) Hepatic and pulmonary tumor load and IGF1R activation in tumor-harboring *Igfbp7*$^{-/-}$ or control mice. Tumor cells were transplanted into the liver or lung of *Igfbp7*$^{-/-}$ or control mice. After the recipient mice were treated with doxorubicin, hepatic and

pulmonary tumor load were analyzed. IGF1R activity was analyzed with immunostaining of pIGF1R; n = 7–10 mice per group. Scale bar = 50 μm.

(**D**) Activation of IGF1R in tumor cell transplanted to WT *Igfbp7*$^{+/+}$ and *Igfbp7*$^{-/-}$ mice with or without chemotherapy. LCs, HCCs, and LLCs were isolated from tumor mass, and p-IGF1R and total IGF1R proteins were assessed by western blot and normalized to β-actin; n = 8–9 mice per group.

(**E**) Survival of tumor-harboring mice was determined after injection of IGF1R neutralizing antibody with or without doxorubicin treatment. n = 12–15 mice per group.

See also Figure S4.

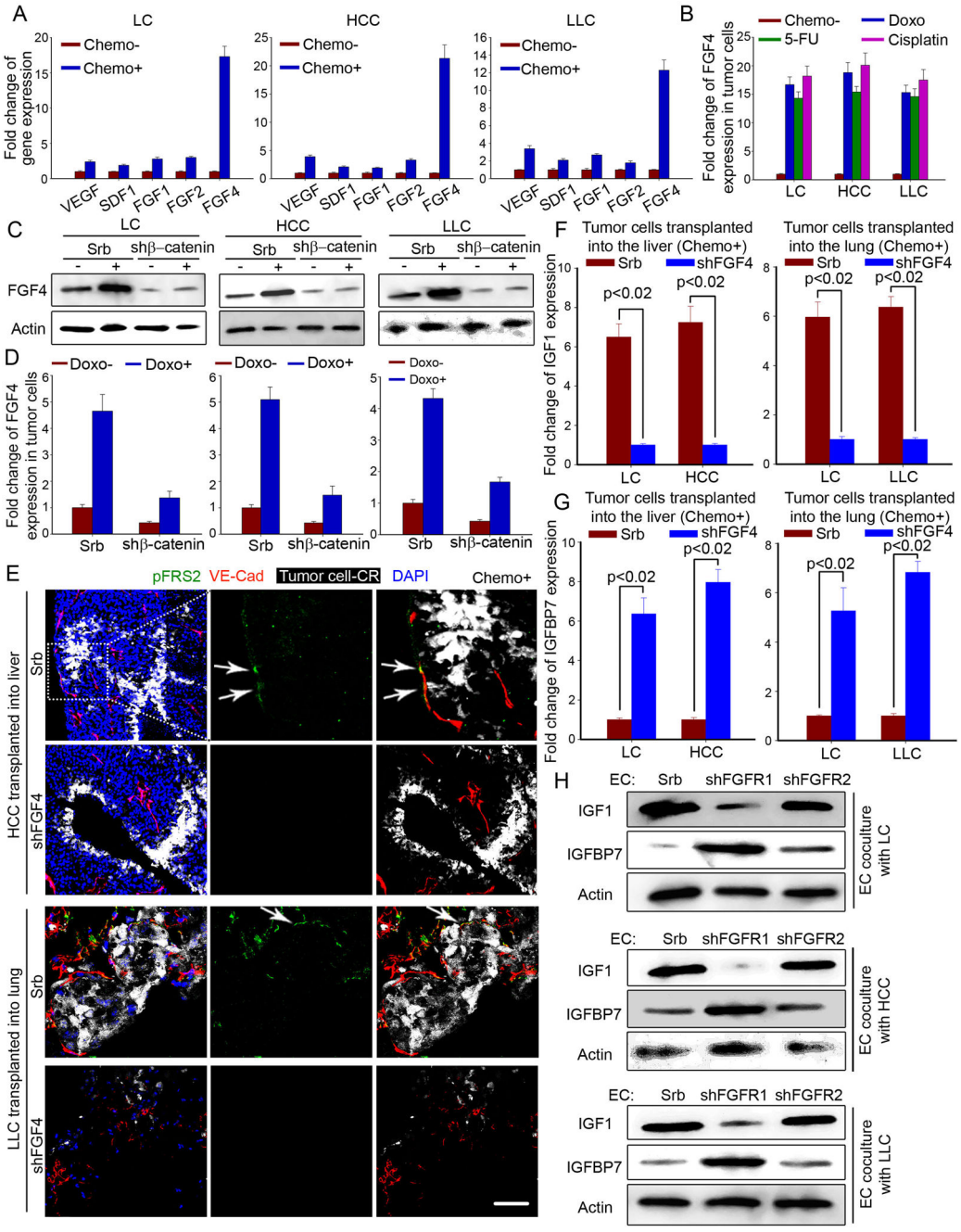

Figure 5. Tumor cell-derived FGF4 modulates the balance between IGF1 and IGFBP7 expression in TECs, augmenting chemoresistance

(**A**) Expression of EC-activating cytokines in tumor cells after treatment with doxorubicin. After cultured tumor cells were treated with doxorubicin, transcriptional expression of indicated growth factors were compared; n = 5 per group.

(**B**) Transcription of FGF4 in indicated tumor cells after treatment of indicated chemotherapeutic agents; n = 4–6 per group.

(**C, D**) After tumor cells were transduced by β-catenin-specific (shβ-catenin) or scrambled (Srb) shRNA, FGF4 protein expression by tumor cells was tested after doxorubicin treatment; n = 4–6 per group.

(**E–G**) FGF4-derived from tumor cells regulates the expression of IGF1 and IGFBP7 in TECs. FGF4 was knocked down in tumor cells by shRNA (shFGF4). shFGF4 or Srb-treated tumor cells were transplanted into the liver or lung of WT mice. FGF-receptor activation in TECs of recipient mice was determined by immunostaining of phosphorylated FRS2 (pFRS2) (E). Transcriptional expression level of IGF1 (F) and IGFBP7 (G) in TECs was measured; Scale bar = 50 μm; n =10–12 mice per group. Tumor cell-CR denotes tumor cells labeled with mCherry red fluorescent protein. Note the localization of p-FRS2 in TECs associated with tumor cells transduced with Srb (arrow) but not shFGF4.

(**H**) FGFR1 and FGFR2 expressions were silenced in HUVECs by shRNA. FGFR1- or FGFR2-deficient HUVECs were incubated with tumor cells, and expression of IGF1 and IGFBP7 in co-cultured HUVECs was analyzed by Western blot; n = 5 per group.

See also Figure S5.

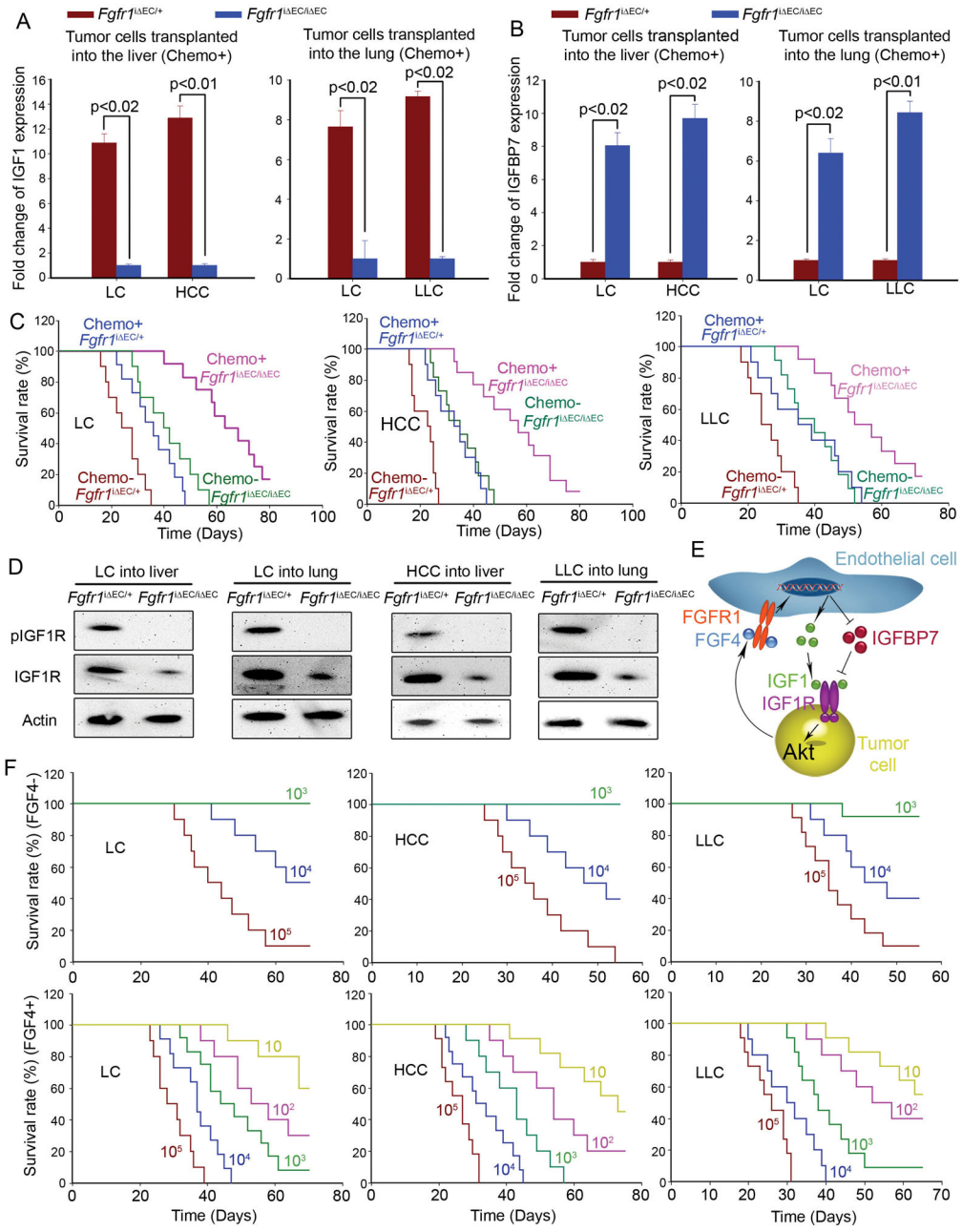

Figure 6. FGFR1 in TECs mediates the effect of FGF4 on IGF1 and IGFBP7 expression

(**A–B**) FGFR1 signaling regulates expression of IGF1 and IGFBP7 in TECs. Tumor cells were transplanted into the liver or lung of mice with EC-specific *Fgfr1* deficiency (*Fgfr1*$^{i\Delta EC/i\Delta EC}$) or control (*Fgfr1*$^{i\Delta EC/+}$) mice by intrasplenic or i.v. injection, respectively. After the recipient mice were treated with doxorubicin, IGF1 and IGFBP7 mRNA level in TECs was measured.

(**C**) Survival of *Fgfr1*$^{i\Delta EC/i\Delta EC}$ and control mice transplanted with indicated tumor cells. LCs and HCCs were i.p. transplanted, and LLCs were i.v. injected into recipient mice, followed by treatment of doxorubicin (Chemo+) or vehicle (Chemo-); n = 10–13 mice per group.

(**D**) IGF1R expression and activation (pIGF1R) in tumor cells transplanted into *Fgfr1*$^{i\Delta EC/i\Delta EC}$ and control mice. Protein level in isolated tumor cells was assayed by Western blot; n = 8 mice.

(**E**) Working model demonstrating that FGFR1 activation in TECs suppresses IGF1R antagonist IGFBP7 and upregulates IGF1, stimulating IGF1R-dependent chemoresistance in tumor cells.

(**F**) Effect of FGF4 on mouse lethality after limiting dilution transplantation of indicated tumor cells. Lethality of injected tumor cells in wild type and *Fgfr1*$^{i\Delta EC/i\Delta EC}$ mice were compared with (FGF4+) or without (FGF4-) injection of FGF4. Indicated numbers of LCs and HCCs were i.p. injected, and LLCs were administered via jugular vein injection; n = 10–14 mice per group.

See also Figure S6.

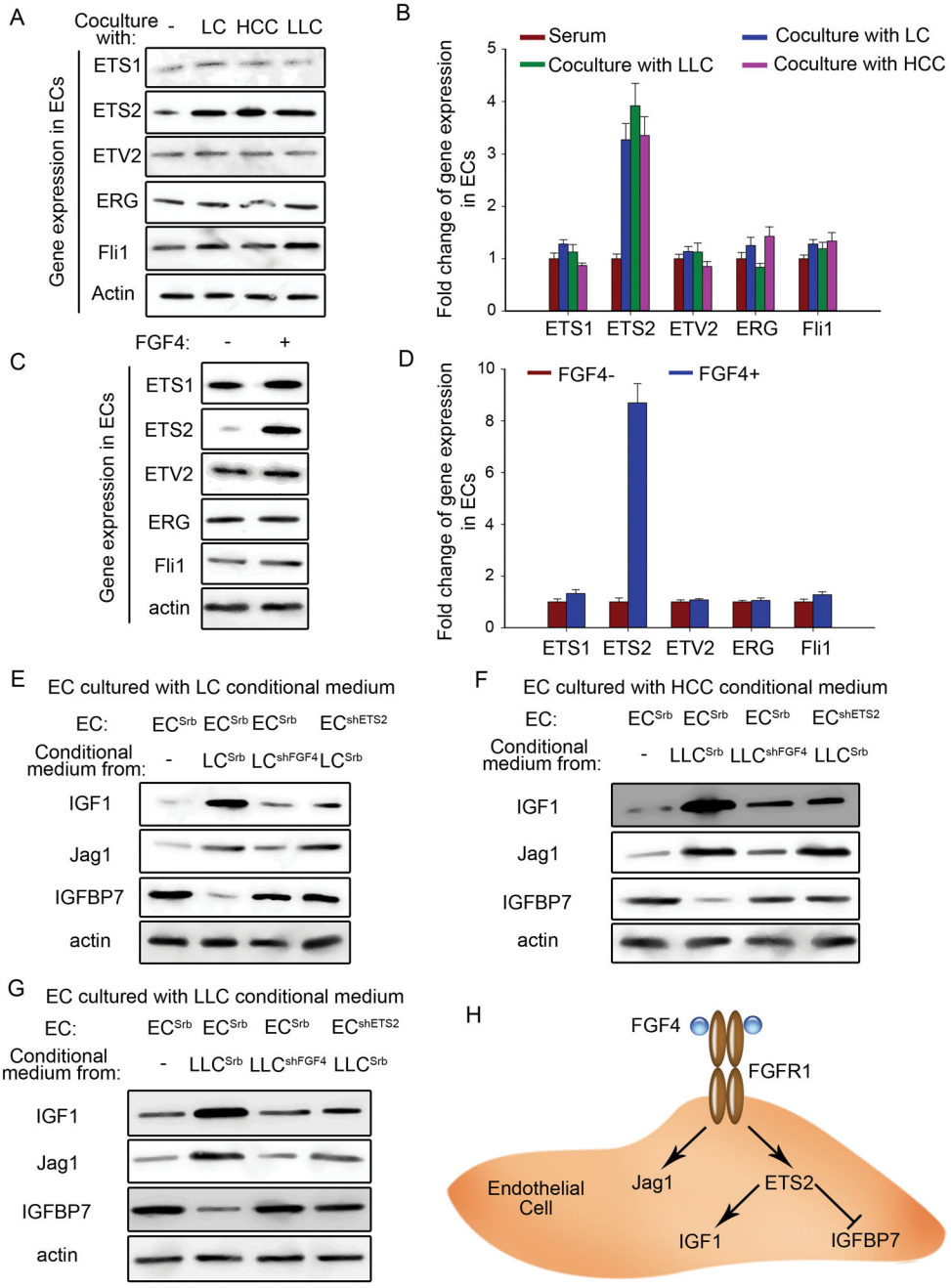

Figure 7. Contribution of ETS2 in FGF4-dependent regulation of IGF1 and IGFBP7 pathways in TECs

(**A–D**) Protein level of E26 transformation-specific (ETS) family transcription factors in HUVECs after FGF4 stimulation (A–B) or incubation with conditioned medium from described tumor cells (C–D); n = 5–6 per group.

(**E–G**) Expression of indicated endothelial paracrine factors in HUVECs after shRNA-mediated ETS2 knockdown in HUVECs or FGF4 silencing in tumor cells. HUVECs were transduced with ETS2-specific shRNA (shETS2), and tumor cells were treated with FGF4-specific shRNA (shFGF4). Srb-transduced cells were used as control; n = 6 per group.

(**H**) Schema describing FGF4 activates endothelial FGFR1, stimulating ETS2-dependent regulation of IGF1 and IGFBP7 expression in the tumor vascular niche.

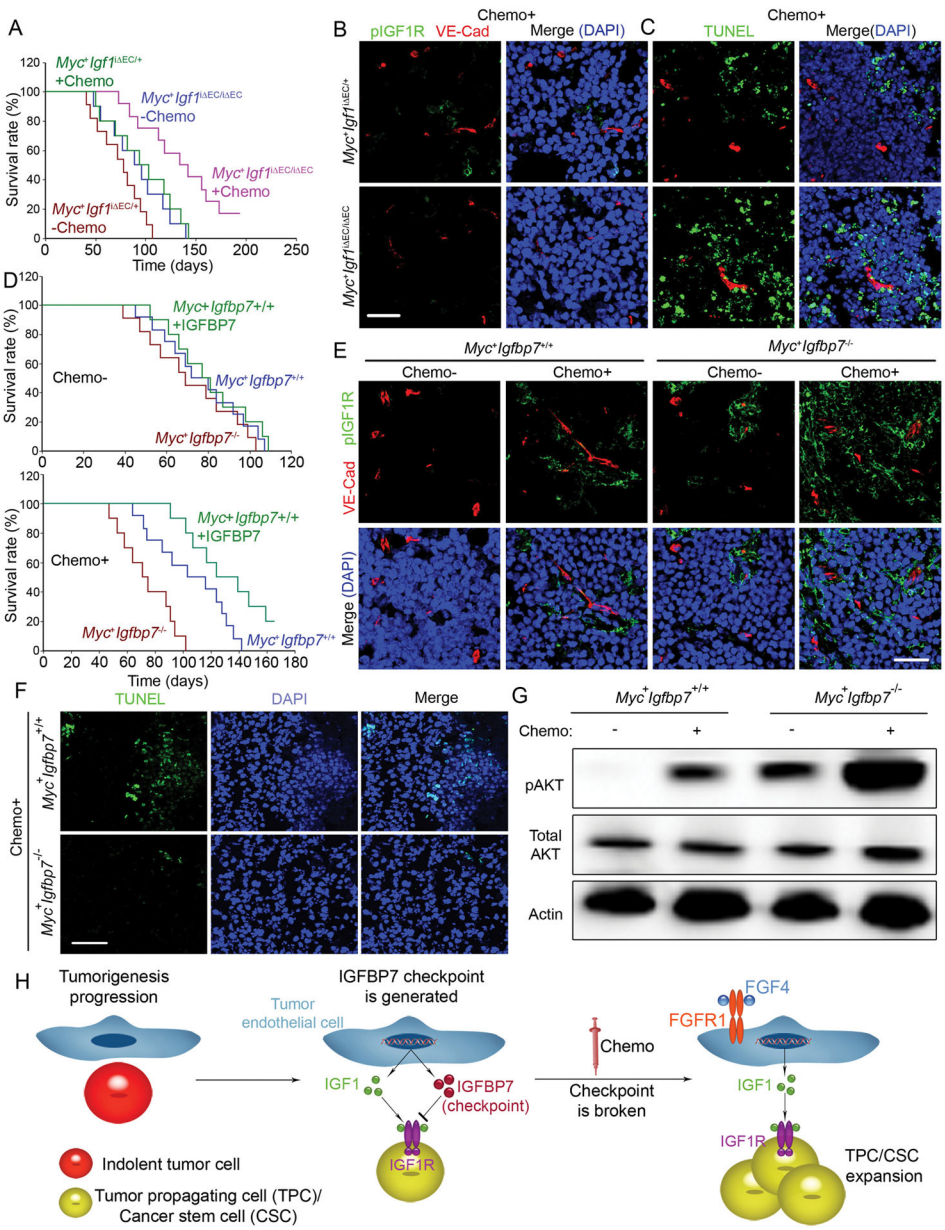

Figure 8. Differential regulation of chemoresistance in *Eμ-Myc* mice by IGF1 and IGFBP7 in TECs

(**A**) *Eμ-Myc* mice were bred with *Igf1*$^{i\Delta EC/i\Delta EC}$ mice. Survival of resultant *Myc*$^{+}$ *Igf1*$^{i\Delta EC/i\Delta EC}$ mice was compared with control *Myc*$^{+}$ *Igf1*$^{i\Delta EC/+}$ mice in the absence (Chemo-) or presence (Chemo+) of doxorubicin-mediated chemotherapy; n = 10–14 mice per group.

(**B**) Activation/phosphorylation of IGF1R in LCs of *Myc*$^{+}$ *Igf1*$^{i\Delta EC/+}$ and *Myc*$^{+}$ *Igf1*$^{i\Delta EC/i\Delta EC}$ mice with doxorubicin treatment (Chemo+). Note the phosphorylation of IGF1R in the perivascular LCs of control mice was absent in *Myc*$^{+}$ *Igf1*$^{i\Delta EC/i\Delta EC}$ mice. Scale bar = 50 um in Figure 8.

(**C**) Cell death in lymphoma mass of $Myc^{+}Igf1^{i\Delta EC/+}$ and $Myc^{+}Igf1^{i\Delta EC/i\Delta EC}$ mice after chemotherapy.

(**D**) *Eμ-Myc* mice were crossed with $Igfbp7^{-/-}$ mice. Survival of generated $Myc^{+}Igfbp7^{+/+}$ and $Myc^{+}Igfbp7^{-/-}$ mice was compared with or without doxorubicin treatment; n = 10–13 mice per group.

(**E**) Phosphorylation of IGF1R (p-IGF1R) in developed LCs of $Myc^{+}Igfbp7^{+/+}$ and $Myc^{+}Igfbp7^{-/-}$ mice.

(**F–G**) Cell death (F) and Akt activation (G) were compared in lymphoma mass of $Myc^{+}Igfbp7^{+/+}$ and $Myc^{+}Igfbp7^{-/-}$ mice after chemotherapy.

(**H**) TECs deploy a core "two-hit" angiocrine mechanism to transform indolent tumors into aggressive and chemoresistant TSCs. In response to tumor development, TECs express paracrine “checkpoint” IGFBP7 to restrain the aggressive features of TSCs. While chemotherapy eradicates the majority of tumor cells, aggressive $IGF1R^{+}$ TSCs supply FGF4 to activate FGFR1-ETS2 axis in TECs, causing suppression of IGFBP7 and upregulation of IGF1 in TECs. Loss of suppressive paracrine checkpoint in TECs instigates cancer stem cell-like features in associated tumor cells such as chemoresistance.

See also Figure S7.